Seismic Data Error Functional: influence of wavelength size structures

Ricardo Felipe Chartuni Cabral da Cruz, André Bulcão, Djalma Manoel Soares Filho, Gustavo Catão Alves, Túlio do Valle Moreira (PETROBRAS)

Abstract

The impact on the seismic response of the variation of physical properties on thin layers depends on the magnitude of the seismic wavelength.

Elastic seismic modeling was used to perform the wavefield propagation, as a tool to simulate the variations in the seismic data due to changes in the physical properties. A traditional data misfit functional was calculated based on these results.

As expected by Aki & Richards` approximation for the reflectivity (1980), it was seen that seismic signal is more sensitive to variations in the compressional velocity and density than in the shear velocity.

Introduction

Seismic resolution limits how one can get earth's physical properties. Its use can help at seismic characterization that depends on how accurate one can identify reflectors and determine the distribution of their relevant properties.

Intuitively, one can say the smaller the body artifact, the more difficult is its recognition on a seismic survey. In fact, the artifact's depth also affects its resolution in the same way.

Jannane *et al.* (1989) investigated which parameters of the earth model are resolved by a typical data set. They reached this determination by perturbing a reference earth model with quasi-sinusoidal perturbations according to the wavelength for the entire model. They concluded that seismic data offers no information on ultra-short wavelengths, which relate to localized impedance contrasts, and that intermediary wavelength are dependant on the offset range, in other words, by increasing the offset, the range of wavelengths that affect the seismic data decreases. Long wavelengths, though, mainly affect the background velocity model and measured traveltimes, allowing the successful use of tomographic inversion.

According to the Aki & Richards` approximation for the reflection coefficient, the variations of different physical properties have distinct impacts on the approximation terms. Therefore, model perturbations were created for compressional and shear velocities, as well as for the density model. The influence of the variation of each of these properties in the seismic data misfit functional was tested separately and in conjunction. This resulted in five independent data sets, one for the reference model, one for each of the studied physical properties and another for all the variations taken together.

Methodology

The presented approach consisted in adding a 10% property variation at a fixed depth and modeling the seismic response for this perturbed model as well as for the reference model. The seismic modeling was based on the 2D elastic wave equation, using a staggered Finite Difference approach (Virieux, 1986 and Levander, 1988).

Different perturbed layer thicknesses were tested, in order to show its effect on seismic response. The sizes of these perturbations were in the range of the source wavelength, considering velocities at the chosen target depth. These varied between $\lambda/16$ and λ.

A split-spread survey was simulated to compare different seismic responses for the proposed models. Within the possible situations, 5 different experiments were modeled: (1) the reference model without perturbations; (2) one model with only compressional velocity perturbation; (3) one model with only shear velocity perturbation; (4) one model with only density perturbation; (5) one model with simultaneous perturbations in all the studied properties.

The model used in this work was a modified 2D VTI velocity model, based on the model provided courtesy of HESS. Modifications included an increase in water depth and extension of the bottom of the model to include the parameter perturbation and a reference horizontal reflector with high acoustic impedance. The perturbation was set at a fixed depth with a vertically varying pattern. The pattern was defined by the vertical seismic resolution obtained from equation 1.

$$\lambda_{ver} = \frac{V}{f}, \qquad (1)$$

where V is the local velocity at the considered depth point and f is the dominant frequency of the data.

To compare the perturbed and reference models we computed the following misfit functional:

$$S = \sum_{t=0}^{t_{max}} \left[P_{ref}(r_0,t) - P_{per}(r_0,t) \right]^2 , \qquad (2)$$

where $P(r_0,t)$ is the pressure wavefield at r_0 and time t and indexes *ref* and *per* refer to reference and perturbed models, respectively.

With the misfit functional in equation 2 calculated, the accumulated misfit for each shot was obtained by summing over the entire offset.

Results

Figure 1 shows the unperturbed model used to calculate the misfit functional. The model is 39.3 km wide and 11.1 km deep, with a reference reflector at z=11 km. Grid spacing is 1.016 meters.

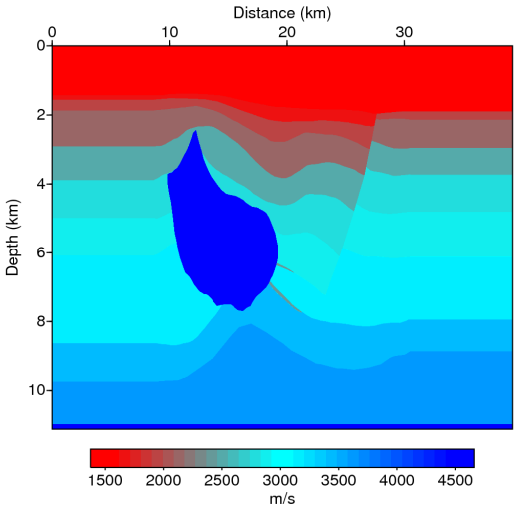

Figure 1: Unperturbed compressional velocity model.

For each of the studied models, the 10% perturbations were added starting at a depth of 9875 meters: one positive followed by one negative variation, with varying thicknesses of *λ/16*, *λ/8*, *λ/4*, *λ/2* and *λ*. The case of a compressional velocity perturbation of size *λ* can be seen in figure 2. Considering an unperturbed compressional velocity of 3620 m/s at the target depth and a dominant frequency of 20 Hz, the perturbed layers in figure 2 are each about 183 meters thick.

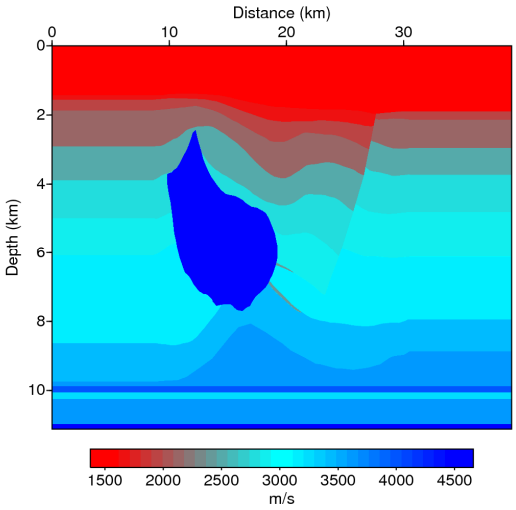

Figure 2: Compressional velocity perturbation with thickness *λ*.

Synthetic seismograms were obtained for shots at coordinates starting at x=1 km up to x=33 km. The seismograms were modeled using the full elastic wave equation, with a maximum frequency of 60 Hz and a calculated dominant frequency of 20 Hz. Receivers were placed in a split-spread configuration with a maximum offset of 6.2 km on each side.

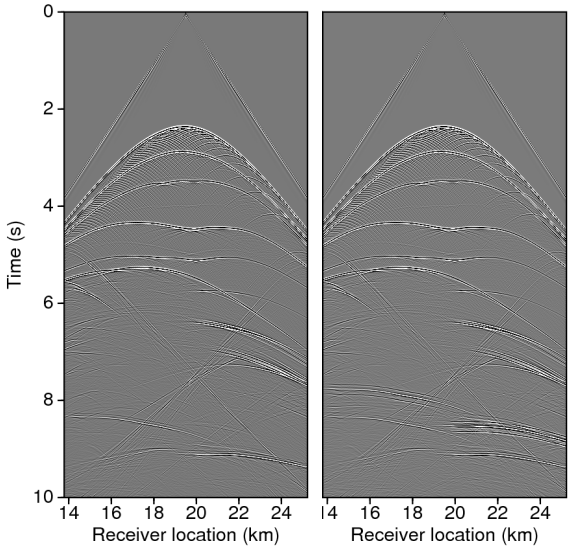

Figure 3: Seismograms for the unperturbed model (left) and *λ* perturbed model (right). Perturbation in this case was for all properties combined.

After generating the seismograms, equation 2 was applied to obtain the misfit functionals for each shot. Figure 4 shows the results for each property and for the different perturbation sizes modeled. Perturbation types numbered 1, 2, 3, 4 and 5 represent thicknesses *λ/16*, *λ/8*, *λ/4*, *λ/2* and *λ*, respectively.

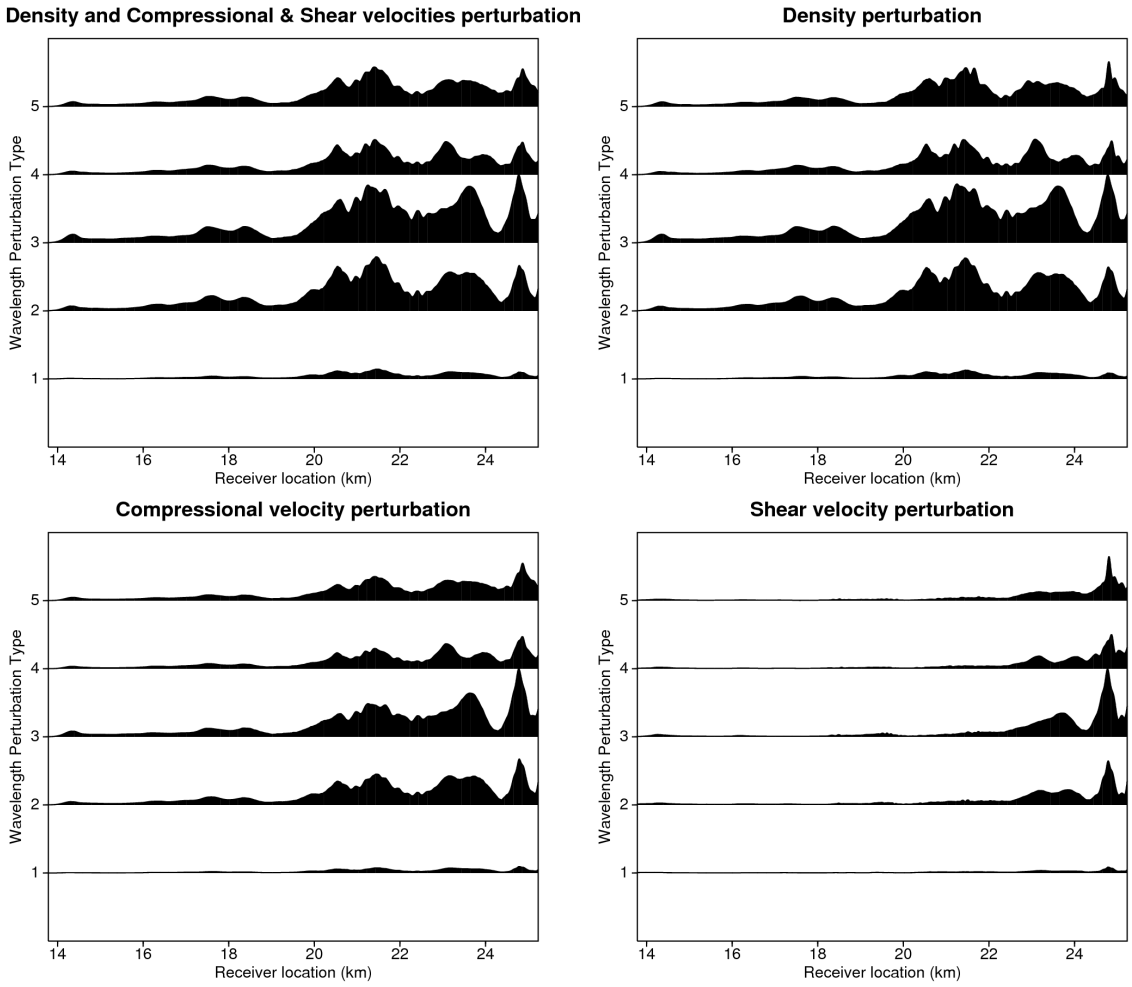

Figure 4: Misfit functionals for each property variation considering the different perturbation sizes. Perturbation types numbered 1, 2, 3, 4 and 5 represent thicknesses *λ/16*, *λ/8*, *λ/4*, *λ/2* and *λ*, respectively.

In the region that corresponds to reflections underneath the salt dome, which correspond to receivers in the 14 - 19 km range, the misfit functional is almost unchanged. This is due to the low illumination of reflectors in this region, according to results by da Silva *et al*. (2011, unpublished).

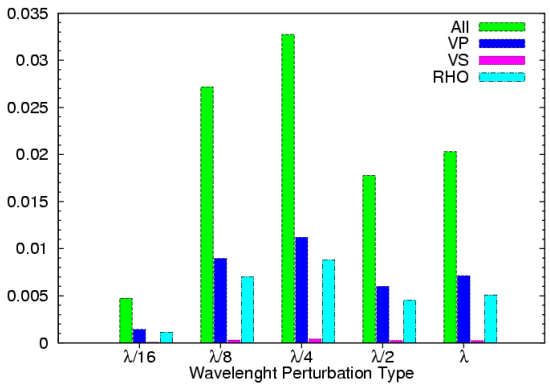

Figure 5: Accumulated misfit functionals for each property variation considering the different perturbation sizes.

The accumulated effect of the perturbation for each property can be obtained by summing over all offsets of a selected shot. These results can be seen in figure 5.

As expected, the combined perturbation of all properties resulted in the strongest variation in seismic response. However, the accumulated misfit functional varies quite differently when each property is perturbed individually. To account for this effect, we must recall the relation between reflectivity and physical properties proposed by Aki and Richards (1980):

$$r \cong \frac{1}{2}\left(\frac{\Delta v_p}{\bar{v}_p}+\frac{\Delta \rho}{\bar{\rho}}\right)-\left(2\frac{\Delta \rho}{\bar{\rho}}\frac{\bar{v}_s^2}{\bar{v}_p^2}+4\frac{\Delta v_s}{\bar{v}_s}\frac{\bar{v}_s^2}{\bar{v}_p^2}\right)sen^2\bar{\theta} + \frac{1}{2}\frac{\Delta v_p}{\bar{v}_p}\tan^2\bar{\theta} \quad , \quad (3)$$

where r is the reflectivity, v_p is the compressional velocity, v_s is the shear velocity, ρ is the density and θ is the incident angle. The bar over the variables indicates an average of the values above and below the interface.

Equation 3 shows that the main contributions to the reflection amplitude in the perturbed model come from the compressional velocity and density variations. The shear velocity component, on the other hand, depends on the square of the sine function of the average incident angle which, for most cases, is very small. The slightly higher values measured for the compressional velocity component could be explained by the third term, which can yield non negligible values for medium incident angles.

Figure 5 also shows how the thickness of the perturbed layer can influence the seismic response. Although the thickening of the layer did produce an increase in the seismic response, there is a sudden decrease in the accumulated misfit when the perturbation changes from $\lambda/4$ to $\lambda/2$. This is due to a tuning effect caused by superposition of the signals from the top and bottom interfaces of the perturbed layer, which is present for layers equal to or smaller than $\lambda/4$. Figure 6 presents a comparison between seismograms showing tuning ($\lambda/16$ $\lambda/8$ and $\lambda/4$) and without tuning ($\lambda/2$ and λ).

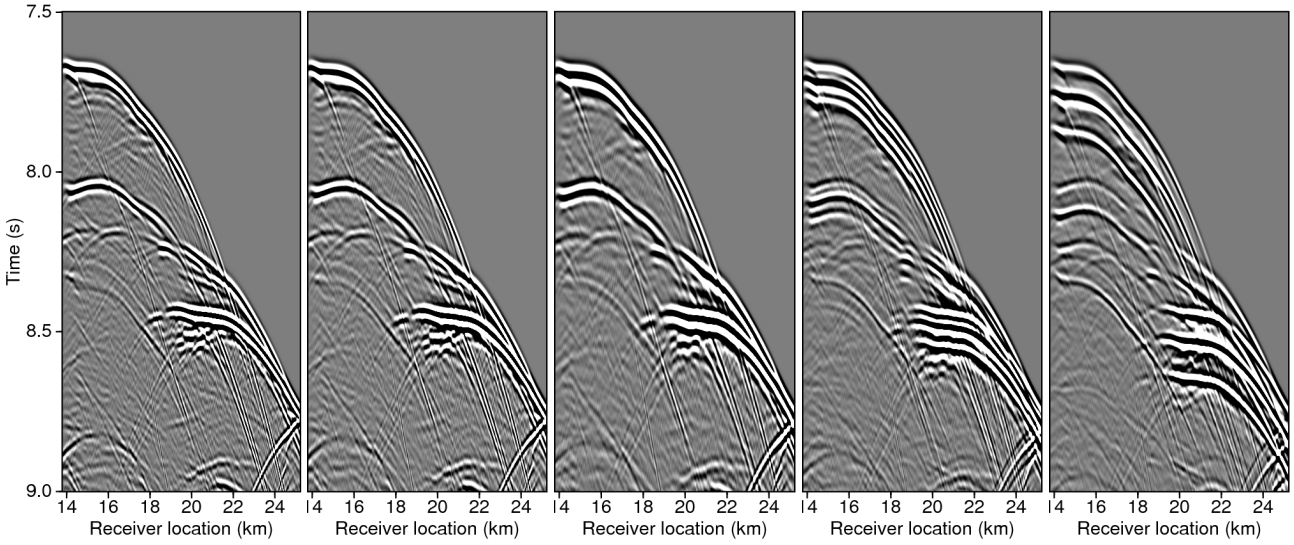

Figure 6: Left to right: superposition of reflected waves for increasing layer thickness ($\lambda/16$ to λ).

Conclusions

It is possible to detect variations of physical properties in layers with thicknesses at the same order of magnitude of the seismic wavelength. However, the seismic signal is more sensitive to variations in the compressional velocity and density than in the shear velocity.

Results agree qualitatively with those expected by applying the Aki & Richards` approximation for reflectivity at small incident angles.

When no deconvolution is applied to the seismogram, tuning effects can influence the results for thin layers. In these cases, care should be taken when analyzing the results.

The presence of a high impedance overburden decreases the amplitudes of the seismic response in this region, making it more difficult to detect variations of the geological physical properties in the misfit functionals in areas with low illumination.

Acknowledgments

The authors would like to thank Petrobras for authorizing this publication.

References

Jannane, M., Beydoun, W., Crase, E., Cao, D., Koren, Z., Landa, E., Mendes, M., Pica, A., Noble, M., Roeth, G., Singh, S., Snieder, R., Tarantola, A., Trezeguet, D. & Zie, M., 1989. Wavelengths of earth structures that can be resolved from seismic reflection data. Geophysics, 54, 906.

Aki, K. & Richards, P.G., 1980. Quantitative Seismology, Theory and Methods. Freeman, S. Francisco.

da Silva, V., Bulcão, A., Mansur, W.J., Alves, G.C., Santos, L.A., Filho, D.J.M., 2011. Qualitative and quantitative illumination analyses using wave equation. Submitted for publication in the 81th SEG.Annual Meeting, Expanded Abstracts.

Levander, A.R., 1988. Fourth-order finite-difference P-SV seismograms. Geophysics, 53, no. 11, 1425.

Virieux, J., 1986. P-SV wave propagation in heterogeneous media: Velocity-stress finite-difference method. Geophysics, 51,889.